

## Nodal surfaces of helium atom eigenfunctions

Tony C. Scott\* and Arne Lüchow†

*Institut für Physikalische Chemie, RWTH Aachen University, 52056 Aachen, Germany*

Dario Bressanini‡

*Dipartimento di Scienze Chimiche e Ambientali, Università dell'Insubria, via Lucini 3, 22100 Como, Italy*

John D. Morgan III§

*Department of Physics and Astronomy, University of Delaware, Newark, Delaware 19716-2570, USA*

(Received 3 October 2006; published 18 June 2007)

Using a rapidly convergent composite basis of Frankowski-Pekeris and Frankowski functions, we have accurately calculated the nodal surfaces of low-lying excited states of the helium atom to investigate Bressanini and Reynolds' conjecture [D. Bressanini and P. J. Reynolds, *Phys. Rev. Lett.* **95**, 110201 (2005)] that these nodal surfaces are rigorously independent of the interelectronic angle  $\theta_{12}$ . We find that in fact there is a slight dependence of the nodal surfaces on  $\theta_{12}$ , but it is so small that the assumption of strict independence may well yield extremely useful approximations in fixed-node quantum Monte Carlo calculations. We explain how Kato's cusp conditions determine the qualitative features of these nodal surfaces, which can accurately be modeled using the familiar ansatz of a symmetric or antisymmetric linear combination of products of hydrogenic orbitals, with some adjustments of the parameters. We explain why a similar near independence of the nodal surfaces on the angular variables can be expected for the ground and singly excited states of the lithium atom, but generally not for larger atoms.

DOI: [10.1103/PhysRevA.75.060101](https://doi.org/10.1103/PhysRevA.75.060101)

PACS number(s): 03.65.Ge, 02.70.Ss

The fixed-node diffusion quantum Monte Carlo method (FN-DMC) [1,2] uses a trial wave function  $\psi$  as a starting point for calculating the exact eigenenergies of a given system. In principle, the accuracy of this method is limited only by the accuracy of the nodes of the trial wave function  $\psi$ . However, exactly determining the nodes of an exact solution of the  $N$ -body Schrödinger wave equation for an excited state of a bosonic system, or even the ground state of a fermionic system with  $N \geq 3$ , has long been elusive.

Recently, Bressanini and Reynolds [3] examined the nodal surfaces of some low-lying excited states of the helium atom, in particular the  $1s2s\ 2^1S$  state and the  $1s3s\ 3^3S$  state. For the  $2^1S$  state, using bases composed of 70 and 203 Hylleraas-type functions, which yield binding energies accurate to 5 or 6 digits, they found that the nodal surface of their approximate wave functions was very nearly independent of the interelectronic angle  $\theta_{12}$ , and they suggested that in the limit of an infinite complete basis, the nodal surface of the exact wave function of this state would be rigorously independent of  $\theta_{12}$ . For the  $3^3S$  state, using a basis of 84 Hylleraas-type functions, they found a nodal surface of qualitatively the same shape, which was also very nearly independent of  $\theta_{12}$ . Furthermore, they suggested this apparent independence of the nodal surfaces on the interelectronic angle might be useful in addressing the fermion sign problem for many-electron systems.

Since the exact  $S$ -state eigenfunctions of the helium atom

are extremely complicated functions of the electron-nucleus distances  $r_1$  and  $r_2$  and a third interelectronic coordinate (either  $r_{12}$  or  $\theta_{12}$ ), it would be surprising if any of the nodal surfaces of these eigenfunctions (besides that at  $r_1=r_2$ , a consequence of spatial antisymmetry under exchange for triplet  $S$  states) were *exactly* independent of  $r_{12}$  or  $\theta_{12}$  [as for the  $^4S(p^3)$  states of a three-electron atomic system [4]]. However, since a singly excited  $S$  state of the helium atom is fairly well described in the independent-electron model by a properly (anti)symmetrized linear combination of products of a  $1s$  hydrogenic orbital for the “inner” electron and an  $ns$  hydrogenic orbital for the “outer” electron, which yields a  $(1s)(ns) \pm (ns)(1s)$  function, which depends on  $r_1$  and  $r_2$  but not on  $r_{12}$  or  $\theta_{12}$ , it should not be surprising that the nodal surfaces of the exact eigenfunctions of such singly excited  $S$  states exhibit only a *weak* dependence on  $\theta_{12}$ . Furthermore, definitively distinguishing such a *weak dependence* of the nodal surfaces on  $\theta_{12}$  from the conjectured *exact independence* of  $\theta_{12}$  requires highly accurate explicitly correlated approximations to the exact excited  $S$ -state eigenfunctions of the helium atom.

Although the Hylleraas-type basis functions employed by Bressanini and Reynolds are mathematically complete as their number tends to infinity [5], expansions in them converge relatively slowly. Composite bases of Frankowski (F) and Frankowski-Pekeris (FP) functions [6], which contain terms that replicate the singularities in the exact nonrelativistic wave functions not only at all three two-particle coalescences [7,8] but also at the three-particle coalescence [9], yield much faster pointwise convergence of both the wave function and its first and second derivatives, which we will evaluate in our analysis below. Variational calculations employing several hundred such F and FP basis functions have

\*scott@pc.rwth-aachen.de

†luechow@pc.rwth-aachen.de

‡Dario.Bressanini@uninsubria.it

§jdmorgan@udel.edu

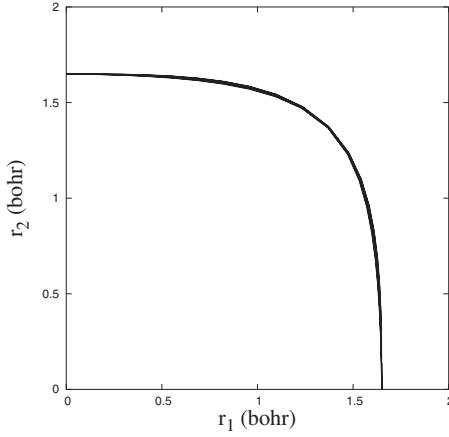


FIG. 1.  $r_1, r_2$  graph of the nodal curves of the  $1s2s 2^1S$  state for  $\theta_{12} = \{\frac{\pi}{6}, \frac{\pi}{3}, \frac{\pi}{4}, \frac{\pi}{2}, \frac{2\pi}{3}, \frac{3\pi}{4}, \pi\}$ .

yielded energies for the ground state and low-lying excited states of helium accurate to 12 or more digits [10,11].

$1s2s 2^1S$  state. The ground state of the helium atom with configuration  $(1s)^2 1^1S$  is nodeless. The lowest excited singlet state of configuration  $1s2s 2^1S$  must have a node so that it is orthogonal to the ground state. In analogy with Fig. 2 of Ref. [3], in Fig. 1 we present plots of the cuts through the nodal surface of this eigenfunction for various values of  $\theta_{12}$ , as determined from highly accurate approximations to the wave function  $\psi$  obtained from large bases of F and FP functions.

The nodal surface of this state is indeed almost independent of  $\theta_{12}$ , but there is a very slight dependence on  $\theta_{12}$  which is most pronounced for  $r_1 \approx r_2$ . To illustrate the excellent convergence of our results, we have superposed the nodal surfaces of  $\psi$  from bases with 265, 291, and 380 F and FP functions, all of which yield an energy of  $E = -2.145 974 046 054 \dots$  a.u. Also superposed are the nodal curves of the Hamiltonian term  $H\psi$  and the kinetic energy term  $T\psi$ , which should coincide exactly with the nodes of  $\psi$  if  $\psi$  is the exact wave function  $\psi_e$ , which obeys  $T\psi_e = (E - V)\psi_e$ . The distances between these nodal surfaces are commensurate with the accuracy of a given wave function [12]. The slight sinusoidal dependence on  $\theta_{12}$ , shown in Fig. 2, can be modeled as a variation from constancy about the midpoint  $\theta_{12} = \pi/2$ , fitted to the approximate form

$$\Delta r = r(\theta_{12}) - r(\pi/2) \approx A \cos(\theta_{12}) + B \cos^2(\theta_{12}). \quad (1)$$

Using a multivariate Taylor series analysis to second order, similar to the first-order scheme used in the Newton-Raphson [12] scheme for finding roots, we find that

$$A = \left. \frac{(\partial\psi/\partial v)}{(\partial\psi/\partial r)} \right|_{v, \Delta r=0}, \quad (2)$$

where  $v = \cos(\theta_{12})$ ,  $r_1 = r_2 = r = 1.3712 \dots$ , and

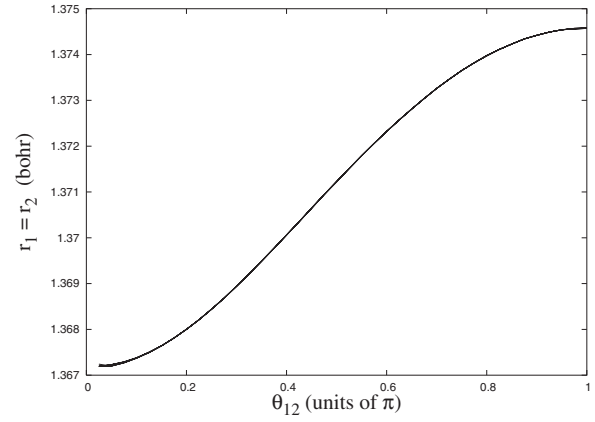


FIG. 2. Point  $r_1 = r_2$  vs  $\theta_{12}$  for the nodal curve of the  $1s2s 2^1S$  state.

$$B = - \left. \frac{\left( \left( \frac{\partial\psi}{\partial r} \right)^2 \frac{\partial^2\psi}{\partial v^2} + \left( \frac{\partial\psi}{\partial v} \right)^2 \frac{\partial^2\psi}{\partial r^2} - 2 \frac{\partial\psi}{\partial v} \frac{\partial^2\psi}{\partial v \partial r} \frac{\partial\psi}{\partial r} \right)}{2 \left( \frac{\partial\psi}{\partial r} \right)^3} \right|_{v, \Delta r=0}$$

and  $\psi$  is the precise wave function. For the  $2^1S$  state, we find  $A = -0.003 65$  and  $B = -0.000 35$ . These values have been confirmed both graphically and by comparison with a least-squares fit. From the distances between the nodal surfaces of  $T\psi$  and  $\psi$  and the Kantorovich theorem [12], we can establish a true bound for the node since the Kantorovich parameter [12]  $h_0 \ll 1$  and consequently the exact node is definitely within the plotting accuracy of the graph shown in Fig. 2. Note that the value of  $A$  depends on the accuracy of  $\partial\psi/\partial v$  at  $r$ , which we find is only  $-0.000 008 624 6$  a.u.

The most precise means of calculating these derivatives is by formally taking partial derivatives of the Schrödinger equation [13]. For the helium atom, these must satisfy the pair of equations

$$(H - E) \left( \frac{\partial\psi}{\partial v} \right) = - \frac{(r_1^2 + r_2^2)}{r_1^2 r_2^2} \frac{\partial\psi}{\partial v} - (\nabla_v V) \psi,$$

$$(H - E) \left( \frac{\partial\psi}{\partial r_j} \right) = - \frac{1}{r_j^3} \frac{\partial^2\psi}{\partial v^2} - \frac{1}{r_j^2} \frac{\partial\psi}{\partial r_j} - (\nabla_{r_j} V) \psi, \quad (3)$$

which are evaluated at  $v=0, \Delta r=0$ .

$1s3s 3^3S$  state. Spatial antisymmetry under exchange requires that the eigenfunctions of all triplet  $S$  states of the helium atom have a nodal plane at  $r_1 = r_2$ , independent of  $\theta_{12}$ . This is the only nodal surface of the  $1s2s 2^3S$  state. The  $1s3s 3^3S$  state has a second nodal surface, qualitatively similar to that of the  $1s2s 2^1S$  state, illustrated in Fig. 3, with the nodal surfaces of  $H\psi$  and  $T\psi$  superposed. Their accuracy was confirmed using composite bases of 265, 380, and 440 F and FP functions, all of which yield an energy of  $E = -2.068 689 067 472 \dots$  a.u. For the case  $r_1 = 2r$  and  $r_2 = r/2$ , a slight sinusoidal dependence on  $\theta_{12}$  is observed, which is qualitatively similar to the behavior of Fig. 2 for the  $2^1S$

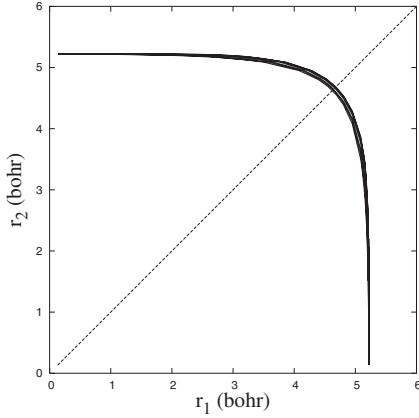


FIG. 3.  $r_1, r_2$  graph of the nodal curves of the  $1s3s\ 3^3S$  state for  $\theta_{12} = \{\frac{\pi}{6}, \frac{\pi}{3}, \frac{\pi}{4}, \frac{\pi}{2}, \frac{2\pi}{3}, \frac{3\pi}{4}, \pi\}$ .

state. For the  $3^3S$  state, we find  $A = -0.002\ 981$  and  $B = -0.000\ 573$ .

$1s2p\ 2^3P^o$  state. We have also examined the conjecture [13,14] that the exact wave function  $\psi_e$  for the  $2^3P^o$  state has the separable form

$$[g(r_1, z_1) - g(r_2, z_2)]\phi(r_1, r_2, r_{12}). \quad (4)$$

From the Breit structures for this  $^3P^o$  state [1, Eq. (1)],

$$\Psi(^3P^o) = z_1 f(r_1, r_2, r_{12}) - z_2 f(r_2, r_1, r_{12}), \quad (5)$$

and pattern-matching between Eqs. (4) and (5) implies

$$z_1 f(r_1, r_2, r_{12}) = g(r_1, z_1)\phi(r_1, r_2, r_{12}), \quad (6)$$

$$z_2 f(r_2, r_1, r_{12}) = g(r_2, z_2)\phi(r_1, r_2, r_{12}). \quad (7)$$

The ratio of Eq. (6) to Eq. (7), which is simply

$$\frac{z_1 f(r_1, r_2, r_{12})}{z_2 f(r_2, r_1, r_{12})} = \frac{g(r_1, z_1)}{g(r_2, z_2)}, \quad (8)$$

should be independent of the Cartesian coordinates  $x_i$  and  $y_i$ , where  $i=1,2$ . However, we find that this ratio has small dependences on these Cartesian coordinates, as shown in Fig. 4. This is shown by transforming the Cartesian coordinates into spherical coordinates and plotting this ratio for specific values of the spherical angles  $\theta_i$  with one of the angles,  $\phi_i$ , held constant, while the other angle  $\phi_j$  varies from 0 to  $2\pi$ . This was done for this  $^3P^o$  state using bases composed of 409 and 533  $P$ -symmetry F and FP functions, which yield an energy  $E = -2.133\ 164\ 190\ 779\dots$  a.u. If the conjecture were true, Fig. 4 should be flat, but we find that it exhibits a small sinusoidal dependence on the spherical angles  $\phi_1$  and  $\phi_2$ .

The qualitative features of the nodal curves in Figs. 1 and 3 near two-particle coalescences are determined by Kato's electron-nucleus cusp condition [7–9]

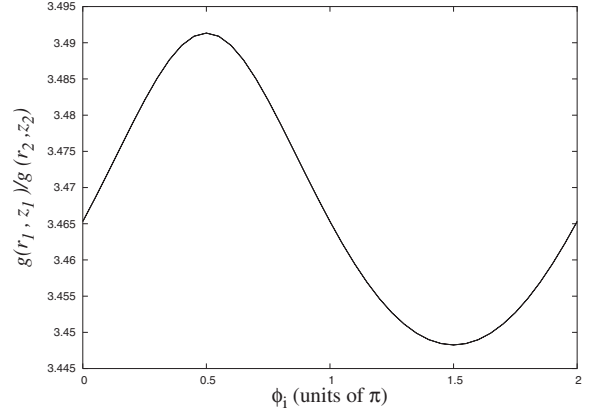


FIG. 4. Superposed plots of the ratio  $g(r_1, z_1)/g(r_2, z_2)$  for the  $1s2p\ 2^3P^o$  state vs the spherical angles  $\phi_i$ , where  $i=1,2$  for  $r_1=1$ ,  $r_2=\frac{1}{2}$ ,  $\theta_1=\theta_2=1$ , and  $\phi_j=\frac{\pi}{2}$ , where  $j \neq i$ .

$$\left. \frac{\partial \langle \psi \rangle}{\partial r_j} \right|_{r_j=0} = -Z\psi(r_j=0), \quad (9)$$

where  $\langle \psi \rangle$  denotes an angular average of  $\psi$  over the surface of a small sphere of radius  $r_j$  centered at  $r_j=0$  and by the associated electron-electron cusp condition for helium  $S$  states,

$$\left. \frac{\partial \psi}{\partial r_{12}} \right|_{r_{12}=0} = \frac{1}{2}\psi(r_{12}=0). \quad (10)$$

At the electron-electron coalescence ( $r_{12}=0$ ), where  $r_1=r_2$  and  $\theta_{12}=0$ , the cusp condition (10) implies that the equation for the nodal surface depends not linearly but quadratically on  $r_{12}$ . Along a node, the right-hand side of cusp condition (9) is zero, so at  $r_j=0$  the partial derivative of the nodal surface with respect to  $r_j$  must also be zero. This explains why the nodal curves for the  $S$  states make right angles with the  $r_1$  and  $r_2$  axes, and are independent of  $\theta_{12}$  at  $r_1=0$  or  $r_2=0$ . Hence, Kato's cusp conditions cause the angular dependence of the nodal surface to vanish at the electron-electron coalescence and the two electron-nucleus coalescences.

To model the nodal curve in Fig. 1, we constructed the simple symmetric function

$$R_{1s}(Z_1, r_1)R_{2s}(Z_2, r_2) + R_{2s}(Z_2, r_1)R_{1s}(Z_1, r_2), \quad (11)$$

where  $R_{1s}$  and  $R_{2s}$  are the hydrogenic  $1s$  and  $2s$  radial functions and  $Z_1$  and  $Z_2$  are arbitrary positive parameters, which can be used to mimic unscreened and/or partially screened nuclear charges. If  $Z_1=Z$  and  $Z_2=Z-1$ , with  $Z=2$  for the helium atom, ansatz (11) yields an independent electron formulation, with the “inner” electron seeing an unscreened nuclear charge of  $Z$  and the “outer” electron seeing a screened nuclear charge of  $Z-1$ , but such a choice for the pair of charges does not accurately reproduce the nodal curve of the  $2^1S$  state. The equation of the nodal curve for ansatz (11) can be solved *exactly* for arbitrary charges  $Z_1$  and  $Z_2$ :

$$r_2 = \frac{2}{Z_2} + \frac{2}{Z_e} W\left(\frac{Z_e p(r_1) e^{-Z_e p(r_1)}}{2Z_2}\right), \quad (12)$$

where  $Z_e = (2Z_1 - Z_2)/(2Z_2)$ ,  $p(r_1) = 2 - Z_2 r_1$ , and the Lambert  $W$  function [15] is the solution of  $W(t)\exp[W(t)] = t$ . Ensuring that the partial derivative of the nodal curve with respect to  $r_1$  is zero, as demanded by Kato's electron-nucleus cusp condition (9), would require that  $Z_1$  and  $Z_2$  have a common value, which we call  $Z_{eff}$ . Kato's cusp condition in itself would demand that  $Z_{eff} = 2$ . However, the resulting node for  $Z_1 = Z_2 = 2$  in ansatz (11) is far from the exact node; e.g., for  $r_1 = r_2 = r$  ansatz (11) vanishes at  $r = 2$ , far from the exact node at  $r = 1.3712$  in Fig. 1. We find that for  $\cos(\theta_{12}) = 0$ , a good fit to the exact node requires that  $Z_{eff}$  continuously varies from 1.46 (at  $r_1 = r_2$ ) to 1.55 (at  $r_1 = 0$  or  $r_2 = 0$ ). This discrepancy between the latter and  $Z = 2$  reflects the varying amount of screening by the inner electron of the effective nuclear charge seen by the outer electron, depending on the relative orientation of the two electrons, which is not reflected in the simple independent-electron ansatz (11).

Proceeding from helium to polyelectronic atoms, the nodal surface of the wave function of the ground state of the lithium atom, with nominal configuration  $(1s)^2(2s)$ , depends very weakly on the angle between the outer electron and either of the two inner core electrons, and the  $(1s)^2$  wave function for the two core electrons is nodeless. Hence, the nodal surface of the ground state of the lithium atom depends only very weakly on the associated angular variables [16]. The same should be true to an even greater extent for singly excited  $S$  states of lithium with nominal configurations  $(1s)^2(ns)$ , with  $n > 2$ .

The exact correlated ground-state wave function of the beryllium atom exhibits strong mixing of the configurations  $(1s)^2(2s)^2$  and  $(1s)^2(2p)^2$ , where the former function has no angular dependence but the latter function contains terms proportional to  $\mathbf{r}_i \cdot \mathbf{r}_j = r_i r_j \cos(\theta_{ij})$ . Hence, the nodal surfaces of this wave function must depend noticeably on the angular variables [16]. Similarly, we expect there to be significant angular dependence in the nodal surfaces of the wave functions of larger atoms, which, in the independent-particle model, have two or more electrons in orbitals with the same value of  $n \geq 2$  and, hence, exhibit strong mixing with other configurations with the same value of  $n$  but different values of  $l$ .

In summary, we have disproved the conjecture that the nodal surfaces of the wave functions of singly excited states of the helium atom (besides that of triplet states at  $r_1 = r_2$ ) are independent of the interelectronic angle  $\theta_{12}$ . We have explained why their dependence on  $\theta_{12}$  is so weak that it might easily be mistaken for independence, and we have explained to what extent analogous behavior of nodal surfaces can be expected in the wave functions of polyelectronic atoms.

Special thanks go to Jonathan D. Baker of NIST for providing highly accurate helium atom wave functions whose generation was supported by NSF Grants Nos. PHY-8317085, PHY-8608155, and PHY-9215442 and a NIST Precision Measurement Award to J.D.M. Financial support by the Deutsche Forschungsgemeinschaft (DFG) in the priority program 1145 is gratefully acknowledged. We also thank Claude Le Sech of the University of Orsay for helpful discussions.

- 
- [1] B. L. Hammond, W. A. Lester, Jr., and P. J. Reynolds, *Monte Carlo Methods in Ab Initio Quantum Chemistry* (World Scientific, Singapore, 1994).
- [2] J. B. Anderson, *J. Chem. Phys.* **65**, 4121 (1976).
- [3] D. Bressanini and P. J. Reynolds, *Phys. Rev. Lett.* **95**, 110201 (2005).
- [4] M. Bajdich, L. Mitas, G. Drobný, and L. K. Wagner, *Phys. Rev. B* **72**, 075131 (2005).
- [5] B. Klahn and W. A. Bingel, *Theor. Chim. Acta* **44**, 9 (1977); **44**, 27 (1977).
- [6] K. Frankowski and C. L. Pekeris, *Phys. Rev.* **146**, 46 (1966); K. Frankowski, *ibid.* **160**, 1 (1967).
- [7] T. Kato, *Commun. Pure Appl. Math.* **10**, 151 (1957).
- [8] W. Kutzelnigg and J. D. Morgan III, *J. Chem. Phys.* **96**, 4484 (1992); J. D. Morgan III and W. Kutzelnigg, *J. Phys. Chem.* **97**, 2425 (1993).
- [9] C. R. Myers, C. J. Umrigar, J. P. Sethna, and J. D. Morgan III, *Phys. Rev. A* **44**, 5537 (1991).
- [10] D. E. Freund, B. D. Huxtable, and J. D. Morgan III, *Phys. Rev. A* **29**, 980 (1984).
- [11] J. D. Baker, R. N. Hill, and J. D. Morgan III, in *Relativistic, Quantum Electrodynamical, and Weak Interaction Effects in Atoms*, AIP Conf. Proc. No. 189 (AIP, New York, 1989), p. 123; J. D. Baker, D. E. Freund, R. N. Hill, and J. D. Morgan III, *Phys. Rev. A* **41**, 1247 (1990).
- [12] A. Lüchow and T. C. Scott, *J. Phys. B* **40**, 851 (2007).
- [13] G. Hadinger, M. Aubert-Frécon, and G. Hadinger, *J. Phys. B* **22**, 697 (1989).
- [14] J. B. Anderson, *Phys. Rev. A* **35**, 3550 (1987).
- [15] T. C. Scott, R. B. Mann, and R. E. Martinez, *AAECC* **17**, 41 (2006).
- [16] D. Bressanini, D. M. Ceperley, and P. J. Reynolds, in *Recent Advances in Quantum Monte Carlo Methods*, edited by W. A. Lester, Jr. (World Scientific, Singapore, 2002), Pt. II, p. 5.